Intelligent Anti-Seismic Foundation: The Role of Fractal Geometry

Ahmad Saoud, Diogo Queiros-Conde, Ahmad Omar, Thomas Michelitsch

buildings

MDPI

Article

Intelligent Anti-Seismic Foundation: The Role of Fractal Geometry

Ahmad Saoud [1,*], Diogo Queiros-Conde [1], Ahmad Omar [2] and Thomas Michelitsch [3]

[1] LEME, Université Paris Nanterre Campus de Ville d'Avray 50, rue de Sèvres, 92410 Ville d'Avray, France
[2] Campus d'Enseignement Supérieur et de Formation Professionnelle, CESI, 93 Bd. de la Seine, 92000 Nanterre, France
[3] Institut Jean le Rond d'Alembert, Sorbonne Université, CNRS UMR 7190, 4 Place Jussieu, CEDEX 05, 75252 Paris, France
* Correspondence: asaoud1991@gmail.com; Tel.: +33-750228476

Abstract: Safe and resistant infrastructure is an essential component of public safety. However, existing structures are vulnerable to damage resulting from excessive ground movement due to seismic activity or underground explosions. The aim of this paper, which is part of an extensive study, is to develop an isolation system based on periodic materials with H-fractal geometry in order to obstruct, absorb or completely modify the pattern of seismic energy before it reaches the foundations of structures. Fractal metamaterial structures have shown promise for increasing the frequency range prohibited for seismic protection. We report the anti-seismic properties of a seismic metamaterial model based on an H-shaped quasi-fractal cell. The fractal design, also known as seismic metamaterials, has an important impact on the band structures of seismic crystals. Using the fractal as a base unit, anti-seismic phononic crystals were developed, and their band-gap characteristics were shown to display unique features due to the increasing wave propagation path and hybridization between local resonances and Bragg scattering. The seismic–mechanical duality is supposed to provide flexible solutions capable of increasing/widening the band-gaps to improve the level of seismic protection.

Keywords: fractal; quasi-fractal; metamaterial; seismic protection; seismic crystals; band-gap; wave propagation

Citation: Saoud, A.; Queiros-Conde, D.; Omar, A.; Michelitsch, T. Intelligent Anti-Seismic Foundation: The Role of Fractal Geometry. *Buildings* **2023**, *13*, 1891. https://doi.org/10.3390/buildings13081891

Academic Editor: Yong Tan

Received: 12 June 2023
Revised: 14 July 2023
Accepted: 23 July 2023
Published: 25 July 2023

1. Introduction

The origins of fractal geometry can be traced to the 19th century [1]. However, in the 1970s, a scientific revolution was launched by Benoit Mandelbrot to develop his fractal geometry [2]. Since then, the applications of fractal structures have been developing more and more, and fractals have been rapidly used in several fields, such as electromagnetics and acoustics, due to their ability to trap elastic/acoustic waves.

The first study, known as a seismic metamaterial, showed the existence of seismic crystals, and it was an experiment on the diffusion of elastic surface waves through a periodic network of cylindrical holes in a marble quarry, which revealed the existence of absolute band-gaps [3]. Subsequently, several seismic crystal studies have been developed. S. Brulé et al. (2014) performed an earthquake experiment using monochromatic Vibro-compaction probe-generated seismic waves, where the velocity measurements of the particles indicated a change in the seismic energy distribution when seismic metamaterials were present [4]. R. Haupt et al. proposed a new system for reflecting and absorbing dangerous seismic waves by creating an artificial underground seismic barrier [5]. M. Miniaci et al. put forward an approach for remote shielding of incoming waves and discussed the feasibility of a passive seismic wave isolation strategy based on large-scale mechanical metamaterials, including numerical analysis of surface and guided waves and the effects of soil dissipation, using full 3D simulations [6].

Bernard Sapoval (Ecole Polytechnique) led a project on multiscale walls borne from fractals in civil engineering. An antinoise wall was directly derived from the physics of

fractals and intended to dampen the noise generated by vehicles on highways [7]. Another civil engineering example is the work of Franck Sgard (2005) of the Habitat Sciences Laboratory (Ecole Nationale des Travaux Publics de l'Etat, Vaulx-en-Velin) [8], where heterogeneous porous materials were designed and proposed for noise control in building and transportation. These materials had multiscale inclusions with a noise damping effect. The use of a fractal system for automotive shock absorbers considerably increases vehicle stability even in the automotive field [9].

Further to fractal structures based on hierarchy, periodic structures (or phononic crystals) that regulate the propagation of waves have been the subject of growing interest for the last 10 years. Phononic crystals have a band-gap; in other words, a particular wave frequency is forbidden. Therefore, their potential technical applications are numerous: elastic/acoustic filters, vibration/noise insulation and seismic control. The unit cell of a phononic crystal consists of an artificial inclusion, void or rigid, covered by the matrix material. Based on most band-gap studies, particularly in seismic isolation, the inclusion consists of regularly shaped geometries such as circles, squares, etc. [10–12]. Recently, several studies have been developed on acoustic and electromagnetic metamaterials in order to study the impact of fractal inclusion on the band structures. Xianfeng Man et al. used the space-coiling approach to obtain an artificial metamaterial for extremely low-frequency airborne sound [13]. J. Liu et al. developed a class of fractal-inspired labyrinthine acoustic metamaterials with hierarchical zigzag channels and highlighted the influences of the self-similar fractal hierarchies on their band structures [14].

Contrary to other fields, such as electromagnetics and acoustics, the applications of fractal structures in seismic crystals are minimal; they can be considered as not yet having been investigated.

In this paper, the self-similar fractal technique is extended to the design of anti-seismic periodic quasi-fractal foundations. The concept of structural hierarchy is applied here in the sense that a unit cell representative of a metamaterial consists of multiple arrangements of inhomogeneities at various size scales. If the same arrangement occurs at every scale, the model is said to be self-similar. In order to study the impact of the H-fractal design on the band structures of the two-dimensional seismic crystal, and looking to create a low-frequency band-gap using fractal geometry, we developed self-similar anti-seismic quasi-fractal structures.

The importance of this model consists of the fact that it is a new type of anti-seismic structural foundation which is simple to implement, low-cost and high-durability [15,16]. We first highlight the concept of fractal seismic crystals or anti-seismic fractal metamaterials and the development of several forms of periodic quasi-fractal foundations. Next, we compare their ability to inhibit the propagation of seismic waves and their band-gap frequencies. Finally, a parametric analysis is carried out to determine the influence of rubber thicknesses and fractal levels on the properties of the attenuation zone.

2. Design and Method of Anti-Seismic H-Shaped Quasi-Fractal Structures

We developed self-similar anti-seismic quasi-fractal structures to create a low-frequency band-gap using fractal geometry. The two-dimensional (2D) unit cells of the first-, second-, third- and fourth-level fractal structures are shown in Figure 1.

We adopted fractal geometry rather than the regular shape geometries applied in most seismic metamaterial studies. As shown in Figure 1, a seismic metamaterial model based on H-shaped quasi-fractal cells was developed. The importance of our study consists of using metal profiles of HEA type that can be easily found on the market without having manufacturing complications, allowing us to build a new type of anti-seismic structural isolator which is simple to realize, with low cost and high durability, which gives originality to our model.

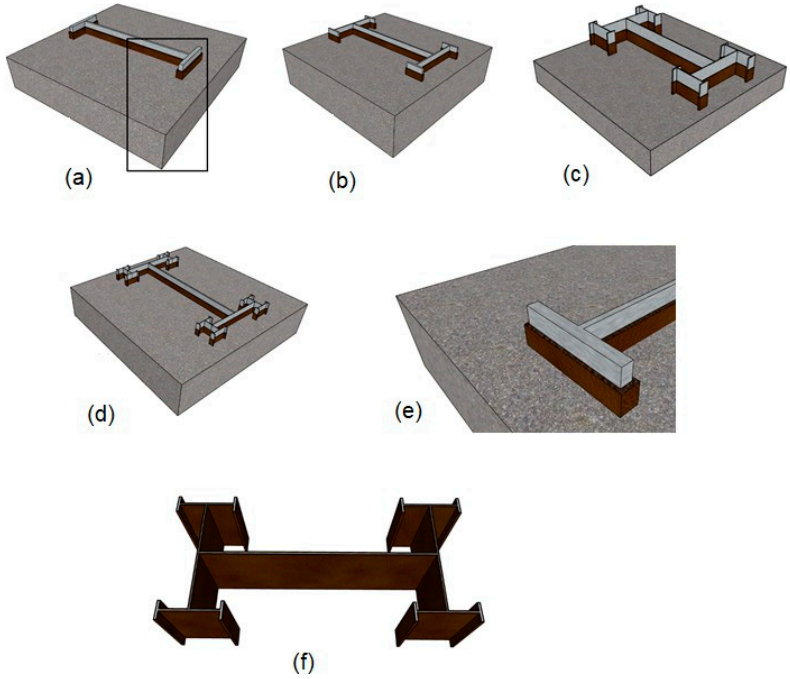

Figure 1. H-SHAPED quasi-fractal up to four levels. (**a**) First level, (**b**) second level, (**c**) third level, (**d**) fourth level, (**e**) zoomed-in section of Figure (**a**), (**f**) H-shaped steel core covered with 2 cm of rubber for third fractal level.

To determine the fractal dimension of an object, it is necessary to count the number of repeated patterns contained in a circle of radius k centered at a given point of the object. This number of patterns is given by $n = k^d$, and the fractal dimension is, therefore, equal to

$$d = \frac{\ln n}{\ln k} \quad (1)$$

The Figure 2 below shows a demonstration of the calculation of the fractal dimension.

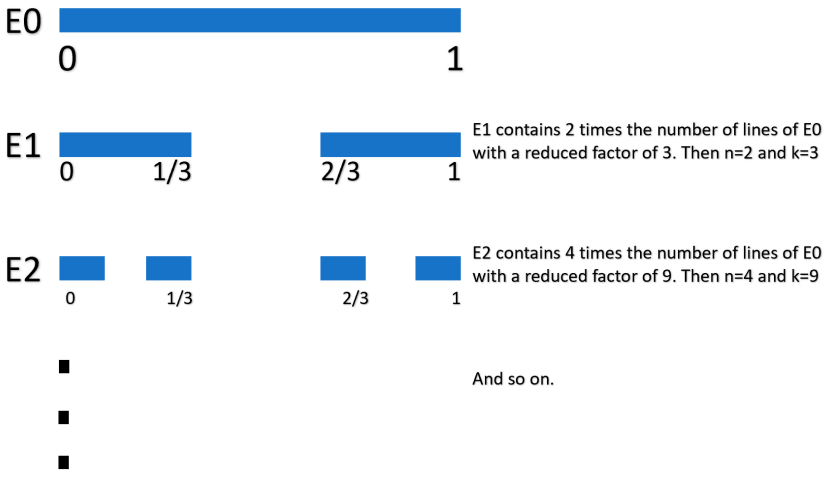

Figure 2. The fractal dimension of the Cantor set d = ln n/ln k = ln 2/ln 3 = ln 4/ln 9 = 0.63.

The first level of the H-shaped quasi-fractal structure is a square unit cell [a (matrix constant) = 1.4 m > h (HEA 1000 profile height) = 0.99 m] consisting of a concrete matrix with H-shaped steel inclusions (HEA 1000) covered with 2 cm of rubber. The number of new small Hs is multiplied for each new fractal level, and the reduced rate of new small Hs is divided. Thus, the second fractal level consists of two smaller H-shaped steel inclusions

(HEA 500) connected by rectangular-shaped pillars. The third and fourth levels are built similarly concerning the overall size of the cell. A self-similar H-fractal structure is achieved by following this process.

Each wrapped steel core is considered as a resonator, where each resonator absorbs wave energy at a frequency range in the anti-resonant frequency range, to reach an equilibrium between the wave and the resonator stresses, where propagation discontinuity is observed.

The finite element method was adopted to calculate the structure's band-gap using Comsol Multiphysics software. The model was studied with a plane deformation, where all parts of the periodic structure were studied in the [X, Y] plane. The periodic structure was modelled in Comsol by implementing a cell and periodic condition according to Bloch's theorem. However, the equations of motion were already implemented in Comsol. Finally, the band structures were calculated using an eigenfrequency analysis.

The fractal dimension D is defined as

$$D = \frac{logN}{log\left(\frac{1}{S}\right)} \tag{2}$$

where:

D: Fractal dimension;
N: Number of auto-similar examples reduced;
S: Reduction factor.

2.1. Material Choice

Local Resonant Phononic Crystals (LRPC) contain an extremely soft elastic material, compared to other materials in the structure, which allows very confined and, therefore, localized vibrational modes to be produced. For this purpose, the selection criterion is the wave propagation speed, which should be lower in the resonators. However, according to Jia Gaofeng and Shi Zhifei's study [17], structures that are made of a steel or lead core are covered with a very soft elastomer. Thus, the effect of the lead core and the elastomer layer (spring) gives the resonator a very localized resonance behavior at very low frequencies.

In our study, we used rubber and steel for the core. The low modulus of elasticity of the rubber and the high mass of the core allowed this type of resonator to withstand low frequencies. In addition to the availability and high mass of the H-shape, its inherent shape, which, combined with the fractal concept, allowed for a very satisfactory level of anti-seismic proofing, was the basis for the design of our H-fractal model. In this study, all materials used were considered as elastic and isotropic materials. The mechanical properties of the materials used in the calculation were ρ = 2450 kg/m^3, E = 28 GPa, ν = 0.2 for concrete; ρ = 7850 kg/m^3, E = 210 GPa, ν = 0.3 for steel and ρ = 1300 kg/m^3, E = 1.37 × 10^{-4} GPa, ν = 0.463 for rubber.

2.2. Periodic Boundary Conditions

The displacements between points of the array to another space in a mesh can be translated by the phase shift of e^{iKbL}. To calculate the band-gaps of a periodic array, we limited the study to an elementary cell by applying the periodic boundary conditions given by Equation (3) below:

$$u(r,t) = e^{i(k\cdot r - wt)}.u_k\left(\overrightarrow{r}\right) \tag{3}$$

where:

K: Wave vector in the reciprocal space;
W: Wave pulsation.

$u_k\left(\overrightarrow{r}\right)$ is on the same periodicity as the elastic parameters, where it satisfies $u_k(r) = u_k(r+L)$.

Thus,

$$\begin{aligned} u(r+L,t) &= e^{i(k(r+L)-wt)} \cdot u_k(r+L) \\ &= e^{ikL} \cdot e^{i(k \cdot r - wt)} \cdot u_k(r) \\ &= u(r,t) \cdot e^{ikL} \end{aligned} \tag{4}$$

2.3. Direct Array and Reciprocal Array

From a geometric point of view, each element of the array illustrated in Figure 3 can be represented using two basic vectors $\vec{d_1}$ and $\vec{d_2}$. Moreover, since the considered array is square geometric, these two vectors define an orthogonal base whose norms are equal to the mesh parameter L:

$$\left\| \vec{d1} \right\| = \left\| \vec{d2} \right\| = L \tag{5}$$

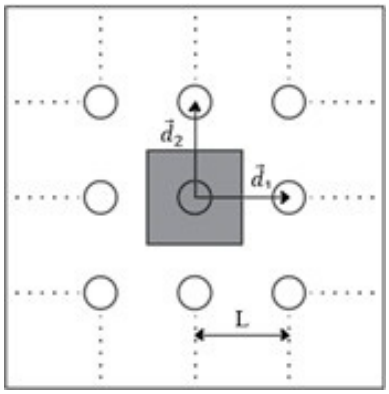

Figure 3. Base vectors and elementary mesh of Wigner–Seitz (gray zone) in the direct array.

Any direct array is associated with a reciprocal array also described by two primary vectors $\vec{r_1}$ and $\vec{r_2}$, as shown in Figure 4 and defined according to the following property:

$$\left\| \vec{r}_1 \right\| = \left\| \vec{r}_2 \right\| = \frac{1}{L} \tag{6}$$

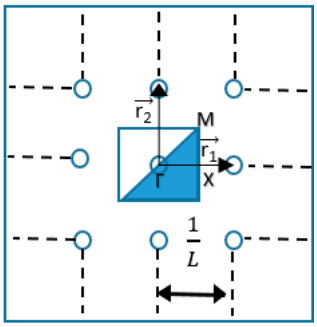

Figure 4. Base vectors and first Brillouin zone in the reciprocal array.

In the particular case of the square array, the two primary vectors of the reciprocal array $\vec{r_1}$ and $\vec{r_2}$ are, respectively, collinear with the primary vectors of the direct array $\vec{d_1}$ and $\vec{d_2}$. The set of points of the reciprocal lattice is described by the vectors $\vec{R}_{m1,\,m2}$ defined by the relation

$$\vec{R}_{m1,m2} = m_1 \vec{r}_1 + m_2 \vec{r}_2 \tag{7}$$

where m_1 and m_2 are relative integers. In the reciprocal lattice, these $\vec{R}$ vectors designate propagation directions. The smallest elementary cell for describing this reciprocal lattice

is called the "first Brillouin zone". This area is delimited by the ΓXM boundary shown in Figure 4.

For the sake of convenience, in the following, the set of points of the reciprocal lattice is described by the vectors $\vec{G}_{m1,m2}$ defined by the relation

$$\vec{G}_{m1,m2} = 2\pi m_1 \vec{r}_1 + 2\pi m_2 \vec{r}_2 \quad (8)$$

2.4. Brillouin Zone

The irreducible Brillouin zone in reciprocal space is equivalent to an array's elementary cell in real space. It is possible to define an elementary cell corresponding to the finite area by the mediating planes between each pattern of the mesh representing the points of high symmetries in the reciprocal lattice.

In the reciprocal space, the basis vectors $\vec{k}_x = \frac{2\pi}{a}\vec{x}$ and $\vec{k}_y = \frac{2\pi}{a}\vec{y}$. The first Brillouin zone is square with $\frac{2\pi}{a}$ as its parameter. The points with high symmetry in this primitive mesh are named Γ, X and M (as shown in Figure 5), and their respective values in the reciprocal array ($\Gamma, \vec{k}_x, \vec{k}_y$) are (0,0), (1/2,0) and (1/2,1/2) [2,18].

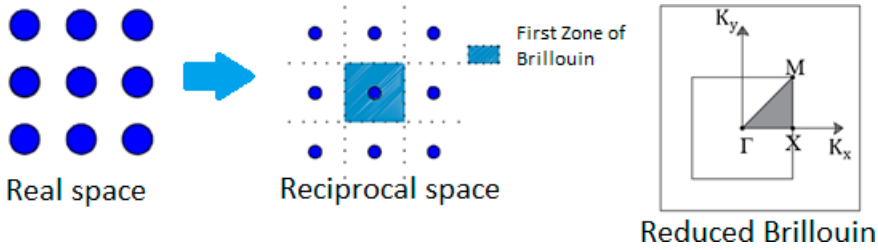

Figure 5. Representation of the square array in a real space and reciprocal space with the first Brillouin zone.

The knowledge of bands' structure in this reduced Brillouin zone is sufficient to know all the methods of propagation in the crystal if we consider it as having infinite periodicity in each direction of the plan.

2.5. Band-Gap Diagram

The propagation of mechanical waves in a medium is usually described by a dispersion relation between the frequency of the wave and the propagation vector (k).

The finite element method was adopted, using Comsol Multiphysics to calculate the band-gap structure. The periodic quasi-fractal structure model was deformed in the [X, Y] plane and modelled by implanting one cell with a periodic condition following Bloch's theorem. The equation of elastic wave propagation in a homogeneous medium (Cheong et al. [19]), presented above (Equations (4) and (5)), had already been implemented in Comsol. Finally, the band structures were calculated using proper frequency analysis:

$$\rho\frac{\partial^2 u_i}{\partial t^2} = \nabla\cdot(\rho C_t^2 \nabla u_i) + \nabla\cdot(\rho C_t^2 \frac{\partial u}{\partial x_i}) + \frac{\partial}{\partial x_i}[(\rho C_l^2 - 2\rho C_t^2)\nabla\cdot u] \quad (9)$$

with C = 1, 2, 3. For a 2D infinite system, the displacement vector $u_i = u(x, y)$, and the equation becomes

$$\rho\frac{\partial^2 u_i}{\partial t^2} = \nabla_T\cdot(C_{44}\nabla_T u_i) + \nabla_T\cdot(C_{44}\frac{\partial u_T}{\partial x_i}) + \frac{\partial}{\partial x_i}[(C_{11} - 2C_{44})\nabla_T\cdot u_T] \quad (10)$$

with $U_T = [u_x, u_y]$ and $\nabla_T = \left[\frac{\partial}{\partial x}, \frac{\partial}{\partial y}\right]$, i = 1, 2.

Bloch's boundary conditions were implanted on the unit cell's exterior edges (Figure 6). Since our importance was in the propagation of seismic waves in the plane X–Y, we used

them to model the periodicity of the cells in the two directions (X, Y). The corresponding equations of Bloch's conditions are

$$U_3 = U_1 \cdot e^{iKxa}$$

$$V_3 = V_1 \cdot e^{iKxa}$$

$$U_4 = U_2 \cdot e^{iKya}$$

$$V_4 = V_2 \cdot e^{iKya}$$

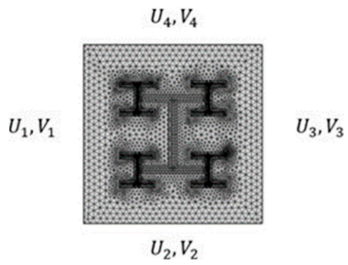

Figure 6. Mesh and periodic conditions of the unit cell.

3. Results

3.1. Impact of H-Shaped Quasi-Fractal Design on the Band Structures

The dispersion curves for different fractal levels are shown in Figure 7. Each unit cell is arranged in a simple square array. The matrix constant a is equal to 1.4 m. This one is maintained constant and equal to the four representative unit cells in order to analyze the effects of the hierarchy on the dispersion of waves in the same frequency range.

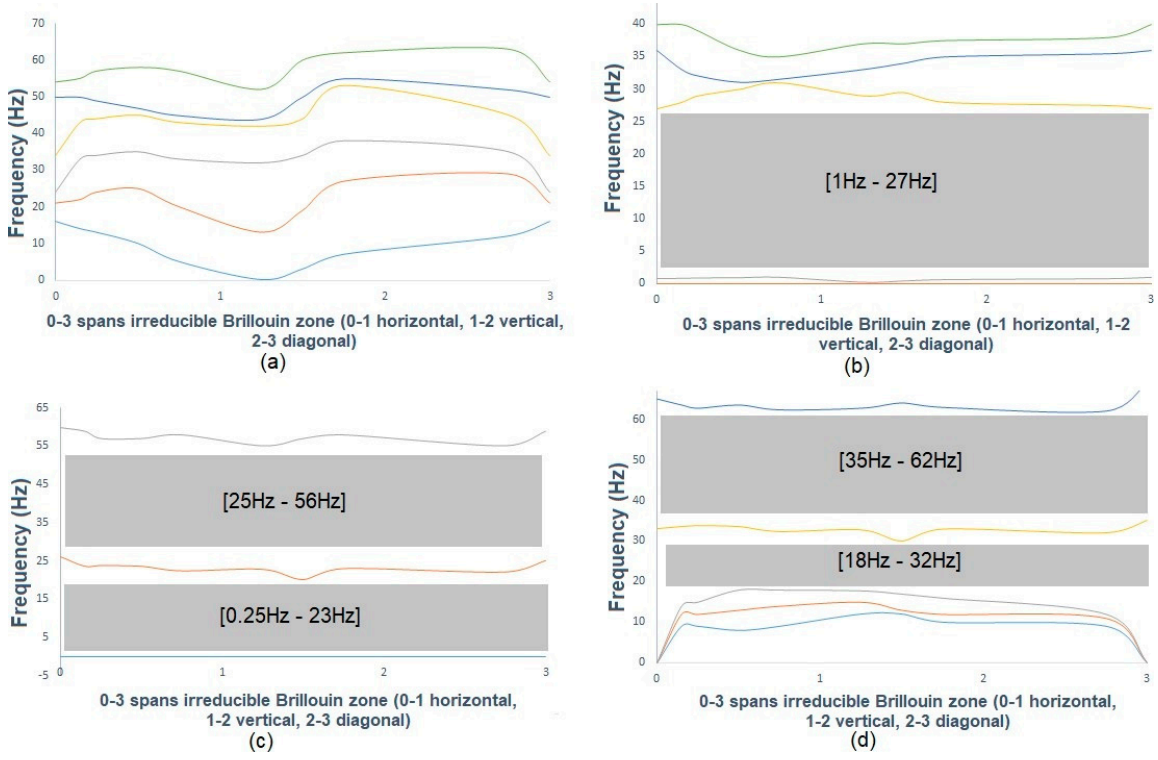

Figure 7. Band structures of an H-shaped fractal structure. (**a**) Band structure of the first fractal level in the frequency range [0 Hz, 100 Hz]. (**b**) Band structure of the second fractal level in the frequency range [0 Hz, 100 Hz]. (**c**) Band structure of the third fractal level in the frequency range [0 Hz, 100 Hz]. (**d**) Band structure of the fourth fractal level in the frequency range [0 Hz, 100 Hz].

The broadband gap frequency from about 1 Hz to 23 Hz was almost preserved for the second and third level fractal structures. However, if we look at the band structures of the different fractal levels in Figure 7, it is easy to observe that, with an increase in the fractal level, the number and proportion of band-gaps in the considered frequency range progressively escalated. Moreover, the results obtained indicate that, by replacing the regular structure with the fractal one, we could significantly increase the bandwidth of the structure by up to 2.5 times without affecting the propagation in the lowest bands for the second- and third-level fractal structures, as shown in Figure 8.

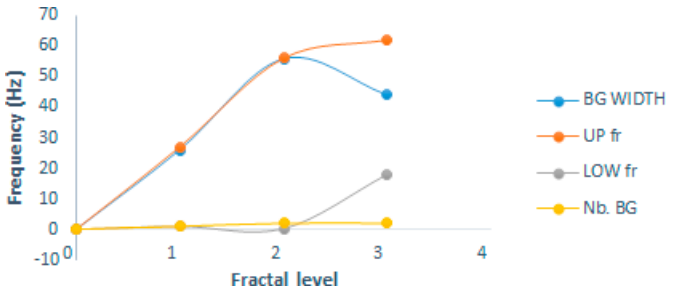

Figure 8. Influence of band-gap's characteristics.

Accordingly, the fractal introduction technique is a practical approach for expanding the band-gap and increasing seismic protection.

3.2. Internal Homothety Effect on Band-Gap Characteristics

The dimension of the internal homothety of fractal structures has been investigated as well. Figure 9 depicts the potential increase in the bandwidth range by reducing the internal homothety of a fractal structure.

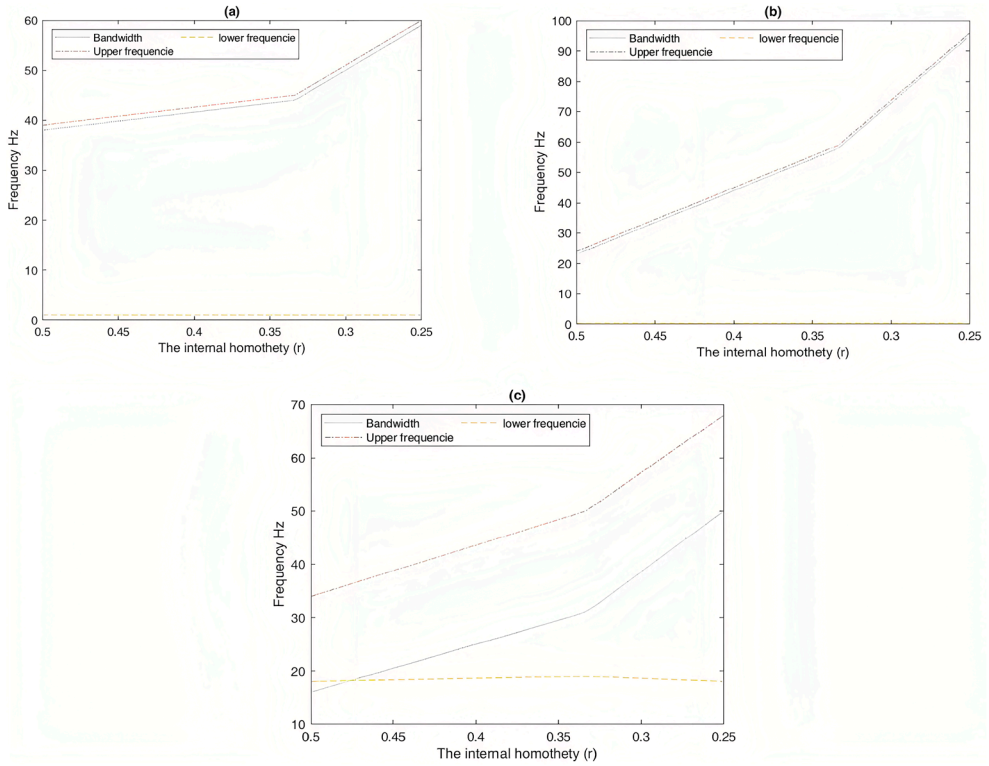

Figure 9. Influence of the dimension of the internal homothety on band-gap's characteristics. (**a**) Second fractal level. (**b**) Third fractal level. (**c**) Fourth fractal level.

Internal homothety of a fractal structure is defined as

$$r(N) = \frac{1}{N} \tag{11}$$

where:

$r(N)$: Internal homothety of a fractal structure;

N: Sub-segment of a fractal structure.

Consequently, we can observe that this increase by up to two times does not affect the propagation in the lowest bands, since the lower band-gap limit is maintained constant, as shown in Figure 9. It is not affected by the change in the internal homothety of a fractal structure.

3.3. Rubber Thickness Effect

After demonstrating the H-shaped quasi-fractal structure as characterized by higher frequency band-gaps, we next analyzed the influence of the rubber thickness on the band-gap property of the H-shaped quasi-fractal structure. The analysis of different thicknesses of rubber for different fractal levels indicated that the presence of rubber was essential, and there was no prominent effect of its thickness on the properties of the frequency band-gaps, as shown in Figure 10. Considering the second and the third fractal levels, for example, they revealed that the lower bond frequency was constant for any rubber thickness, while the upper bond frequency (UBF) of the band-gap was slightly increased, perhaps negligibly, with increasing rubber thickness.

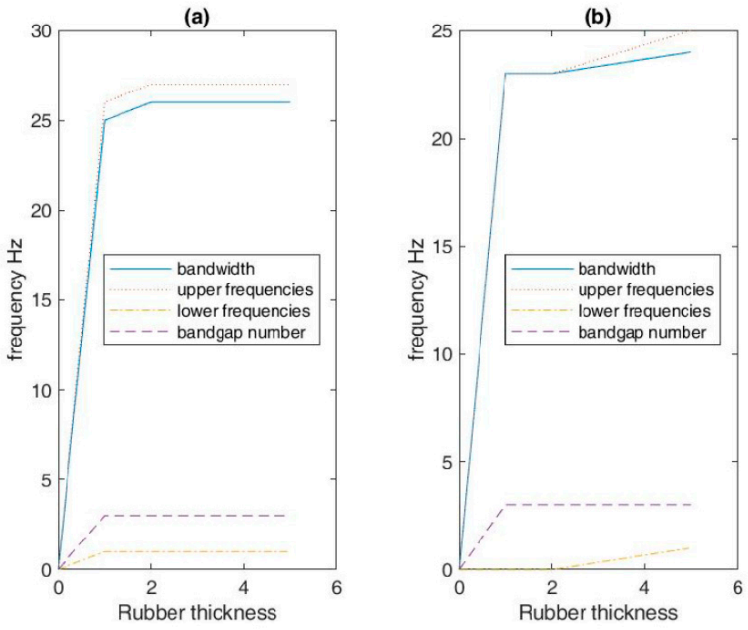

Figure 10. Influence of rubber thickness on band-gap's characteristics. (**a**) Second fractal level. (**b**) Third fractal level.

Thus, the presence of minimum-thickness rubber in our anti-seismic metamaterial based on fractal geometry is the first gateway to open the band-gap for elastic waves. It helps create mechanical resonators and locally resonant band-gaps at each fractal level.

4. Discussion

The critical change in the band structure is explained by the fact that, with the higher-order fractal, the seismic wave travels along a longer spatially winding propagation path

generated by the fractal structure, compared to lower-order fractals. The propagation path equation of the unit cell can be expressed as

$$Lf = \left(\frac{N}{r}\right)^{n} \cdot a \tag{12}$$

where:

Lf: Length of the propagation path;
N: Number of auto-similar examples reduced;
r: Internal homothety of a fractal structure;
a: Matrix constant.

Another reason for this result is that, in the proposed metamaterial H-quasi-fractal structures, a periodic elastic lattice with stiffer regions is introduced due to hierarchical refinement. As a result, the band-gaps of the Bragg type are generated. In addition, each fractal level acts itself as a mechanical resonator, which leads to forming locally resonant band-gaps.

Figure 7d demonstrates that the lacunarity effect is vital in wave propagation at the fourth fractal level. At this level, the bandwidth increases, but we lose a part of the bandwidth at low frequencies. Lacunarity can be defined as a complementary measure of the fractal dimension. It characterizes the connectivity and material distribution properties in the fractal structure. The measures of lacunarity can be used to describe the filling characteristics of data that supply the space [20]. Statistically, this can be simplified by recognizing that lacunarity is the ratio of the variance of the number of groups per cell to the square of the mean plus one [21]:

$$L = \frac{\text{variance(s)}}{mean(s)^2} + 1 \tag{13}$$

5. Verification of the Effectiveness of the Periodic Foundation with H-Shaped Quasi-Fractal Anti-Seismic Metamaterial

A comparative study between traditional concrete foundations and quasi-fractal composite foundations is necessary to verify the effectiveness of periodic foundations with the quasi-fractal anti-seismic H-shaped metamaterial. For this reason, two models were developed with the same upper concrete structure but with different foundations. The first one had a traditional concrete foundation and the second one had a quasi-fractal composite foundation. Each foundation had dimensions of 3.5 m × 7 m × 0.4 m, and the upper structure was formed by frames, where the columns had sections of 0.25 m × 0.19 m and beams of 0.2 m × 0.3 m. These frames were composed of two floors, where each had flat dimensions of 3 m × 3.2 m and a height of 2.9 m.

The fundamental frequency of the upper structure was 5.04 Hz, so the band-gap of the cell was required cover its fundamental frequency. In our case, the cells of the periodic foundation had a thickness of 0.4 m. The properties of the second-level fractal structures gave a bandwidth between 1 and 23 Hz. The finite element method was adopted for the calculation of the vibration response of the 3D structural model, using Comsol Multiphysics 5.3.a. The models were studied by using a time-dependent study.

The displacement conditions were as follows:

- Zero displacement for all points at Z = 0 in the Z direction;
- Vibration amplitude of 5 cm, with different frequencies for all points at Y = 0 in the Y direction.

In this study, we chose a triangularly shaped mesh for the upper structure and the traditional concrete foundation, and a square cylindrical shape, where the sweep direction was parallel to the Z direction, for the quasi-fractal composite foundation, because the stresses and deformations were nearly constant in the Z direction, and, thus, we could use this type of mesh to reduce the computation time.

The convergence of the calculation depends on the size of the elements and the time step (Δt). Using the default value Δt = 0.01 s from Comsol and the above meshes, the calculations converged.

Figure 11 demonstrates the effectiveness of the quasi-fractal composite foundation in the seismic isolation, where it gave a reduction factor of about five inside the band-gap, Since the steel and the concrete matrix oscillated in anti-phase in the steel's anti-resonance frequency range, the energy assembled in the resonators approached the equilibrium between their stresses and wave stresses; thus, the amplitude decreased.

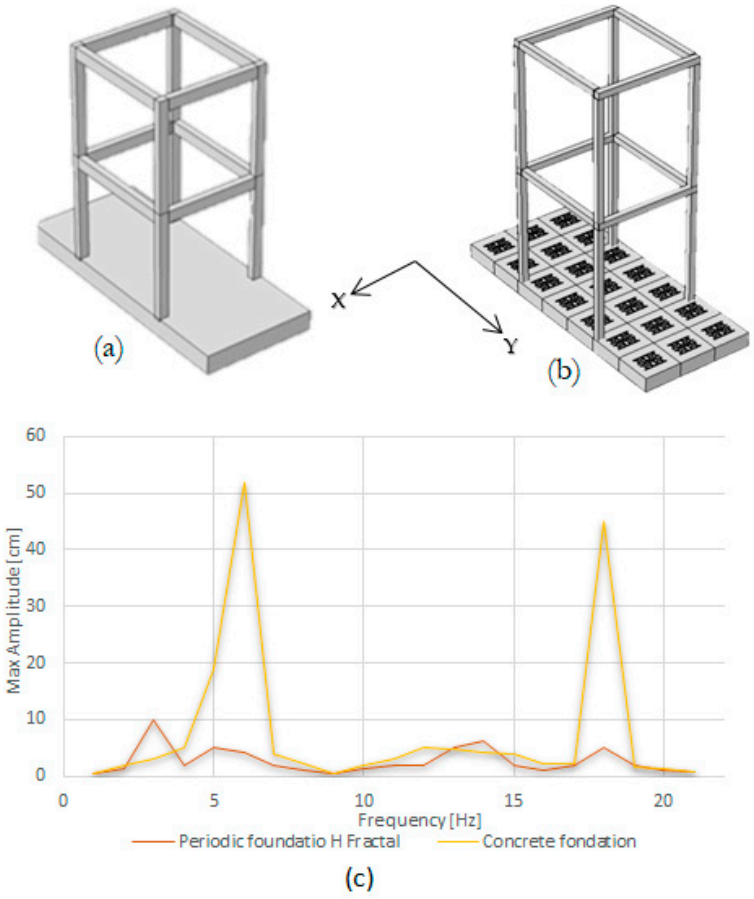

Figure 11. (**a**) Responses of the upper structure with quasi-fractal composite foundation at 5.39 Hz. (**b**) Responses of the upper structure with traditional concrete foundation at 5.4 Hz. (**c**) Maximum relative displacement responses of traditional concrete foundation and quasi-fractal composite foundation.

Since the upper structure acted as a resonator, the efficiency of the range of frequencies—located between the fundamental frequency of the upper structure and the resonance frequency of the resonators—was related to the mass of the periodic foundation's resonators relative to the mass of upper structure. Where the efficiency of the band-gap increased, the mass of resonators increased relative to the mass of the upper structure, because there exists in this range of frequencies a collision between the amplification band due to the upper structure and the band-gap due to the resonators.

6. Conclusions

The results of this research are an important step towards the goal of creating an anti-seismic structure using anti-seismic metamaterials based on fractal geometry to effectively protect structures from seismic waves and explosions.

This work has numerically investigated the anti-seismic properties of an anti-seismic metamaterial structure based on H-shaped quasi-fractal geometry. Contrary to previous approaches, our study focuses on hierarchical structures that highlight several advantages:

1. Maintenance of most BGs induced by the regular constitutive geometries with damping materials;
2. As the hierarchy of the self-similar fractal increases, the bandwidth of the total band-gaps increases progressively by up to 2.5 times, while the lowest band-gaps remain constant.

The dimension of the internal homothety of fractal structures is discussed, and the generality of the displacement behavior is numerically tested. We have also analyzed the effect of rubber thickness on wave propagation in hierarchical metamaterials, establishing their crucial role, even when they are tiny, in preserving the BG size.

The results of this study represent an important step to develop an anti-seismic structure using anti-seismic metamaterials based on fractal geometry to effectively protect the structures from seismic waves. Numerical studies were carried out to verify the band-gap characteristics of the developed fractal models. Therefore, a detailed study of structural stability and bearing capacity of periodic foundations is strongly recommended, which could lead to their design for different structures.

Author Contributions: Conceptualization, A.S., D.Q.-C., A.O. and T.M.; methodology, A.S. and D.Q.-C.; software, A.S. and A.O.; validation, D.Q.-C. and T.M.; formal analysis, A.S., T.M., D.Q.-C. and A.O.; writing—original draft preparation, A.S.; writing—review and editing, A.S. All authors have read and agreed to the published version of the manuscript.

Funding: This research received no external funding.

Data Availability Statement: Not applicable.

Conflicts of Interest: The authors declare no conflict of interest.

References

1. Kummer, E.E. Über die Ergänzungssätze zu den allgemeinen Reciprocitätsgesetzen. *J. Reine Angew. Math.* **1852**, *44*, 93.
2. Mandelbrot, B.B. *Fractals, Form, Chance, and Dimension*; Springer: New York, NY, USA, 1978.
3. Meseguer, F.; Holgado, M.; Caballero, D.; Benaches, N.; Sánchez-Dehesa, J.; López, C.; Llinares, J. RayleighRayleigh-wave attenuation by a semi semi-infinite two two-dimensional elastic elastic-bandband-gap crystal. *Physical. Rev. B* **1999**, *59*, 12169. [CrossRef]
4. Brûlé, S.; Javelaud, E.H.; Enoch, S.; Guenneau, S. Experiments on Seismic Metamaterials: Molding Surface Waves. *Phys. Rev. Lett.* **2014**, *112*, 133901. [CrossRef] [PubMed]
5. Haupt, R.; Liberman, V.; Rothschild, M. Seismic Barrier Protection of Critical Infrastructure from Earthquakes. In Proceedings of the 2017 IEEE International Symposium on Technologies for Homeland Security (HST), Waltham, MA, USA, 25–26 April 2017.
6. Miniaci, M.; Krushynska, A.; Bosia, F.; Pugno, N.M. Large scale mechanical metamaterials as seismic shields. *New J. Phys.* **2016**, *18*, 083041. [CrossRef]
7. Sapoval, B.; Filoche, M.; Chappat, M.; Peyrard, D. Noise Abatement Wall. Mur Antibruit. EP 1488043 B1, 6 November 2013.
8. Bécota, F.-X.; Sgard, F. Laboratoire des Sciences de l'Habitat, DGCB URA CNRS 1652, Ecole Nationale des Travaux Publics de l'Etat, 69518 Vaulx-en-Velin Cedex, France.
9. Le Méhauté, A.; Nigmatullin, R.; Nivanen, L. *Flèches du Temps et Géométrie Fractale*; Hermes Science Publications: Paris, France, 1998.
10. Achaoui, Y.; Ungureanu, B.; Enoch, S.; Brûlé, S.; Guenneau, S. Seismic waves damping with arrays of inertial resonators. *Extrem. Mech. Lett.* **2016**, *8*, 30–37. [CrossRef]
11. Brûlé, S.; Javelaud, E.; Enoch, S.; Guenneau, S. Seismic metamaterial: How to shake friends and influence waves? *arXiv* **2013**, arXiv:1301.7642.
12. Oudich, M. Contribution à L'étude des Cristaux Phononiques à Résonance Locale dans les Régimes Sonique et Hypersonique: Approches Théorique et Expérimentale. Ph.D. Thesis, Université Henri Poincaré, Nancy, France, 2011.
13. Man, X.; Liu, T.; Xia, B.; Luo, Z.; Xie, L.; Liu, J. Space-coiling fractal metamaterial with multi-bandgaps on subwavelength scale. *J. Sound Vib.* **2018**, *423*, 322–339. [CrossRef]
14. Liu, J.; Li, L.; Xia, B.; Man, X. Fractal labyrinthine acoustic metamaterial in planar lattices. *Int. J. Solids Struct.* **2018**, *132*, 20–30. [CrossRef]

15. Nakamura, T. Strength and deformability of H-shaped steel beams and lateral bracing requirements. *J. Constr. Steel Res.* **1988**, *9*, 217–228. [CrossRef]
16. Kato, B. Rotation capacity of H H-section members as determined by local buc kling. *J. Constr. Steel Res.* **1989**, *13*, 95–109. [CrossRef]
17. Jia, G.; Shi, Z. A new seismic isolation system and its feasibility study. *Earthq. Eng. Eng. Vib.* **2010**, *9*, 75–82. [CrossRef]
18. Van Der Biest, F. Diffusion Multiple et Renversement du Temps Ultrasonore dans des Milieux Périodiques et Désordonnés. Ph.D. Thesis, Université de Paris, Paris, France, 7 January 2006.
19. Cheong, Y.K.; Gorishnyy, T.; Thomas, E.L. Phononic Band Structures of Twodimensional Hypersonic Phononic Crystals. In Proceedings of the COMSOL Conference 2007, Boston, IL, USA, 4–6 October 2007.
20. Halley, J.M.; Hartley, S.; Kallimanis, A.S.; Kunin, W.E.; Lennon, J.J.; Sgardelis, S.P. Uses and abuses of fractal methodology in ecology. *Ecol. Lett.* **2004**, *7*, 254–271. [CrossRef]
21. Plotnick, R.E.; Gardner, R.H.; O'Neill, R.V. Lacunarity indices as measures of landscape texture. *Landsc. Ecol.* **1993**, *8*, 201–211. [CrossRef]